THE ASTROPHYSICAL JOURNAL, 478:516–521, 1997 April 1

ULTRAVIOLET IMAGING OBSERVATIONS OF THE cD GALAXY IN ABELL 1795: FURTHER EVIDENCE FOR MASSIVE STAR FORMATION IN A COOLING FLOW

ERIC P. SMITH
Laboratory for Astronomy and Solar Physics, Code 681, NASA Goddard Space Flight Center, Greenbelt, MD 20771; esmith@hubble.gsfc.nasa.gov

RALPH C. BOHLIN
Space Telescope Science Institute, Homewood Campus, Baltimore, MD 21218

G. D. BOTHUN
Department of Physics and Astronomy, University of Oregon, Eugene, OR 97403

ROBERT W. O'CONNELL
Astronomy Department, University of Virginia, Charlottesville, VA 22903

MORTON S. ROBERTS
National Radio Astronomy Observatory, Edgemont Road, Charlottesville, VA 22903

AND

SUSAN G. NEFF, ANDREW M. SMITH, AND THEODORE P. STECHER
Laboratory for Astronomy and Solar Physics, Code 680, NASA Goddard Space Flight Center, Greenbelt, MD 20771
Received 1996 June 24; accepted 1996 October 24

ABSTRACT

We present images from the Ultraviolet Imaging Telescope (UIT) of the Abell 1795 cluster of galaxies. We compare the cD galaxy morphology and photometry of these data with those from existing archival and published data. The addition of a far-UV color helps us to construct and test star formation model scenarios for the sources of UV emission. Models of star formation with rates in the range ~ 5–$20\ M_{\odot}\ \mathrm{yr}^{-1}$ indicate that the best-fitting models are those with continuous star formation or a recent (~ 4 Myr old) burst superimposed on an old population. The presence of dust in the galaxy, dramatically revealed by *Hubble Space Telescope* images, complicates the interpretation of UV data. However, we find that the broadband UV/optical colors of this cD galaxy can be reasonably matched by models using a Galactic form for the extinction law with $E_{B-V} = 0.14$. We also briefly discuss other objects in the large UIT field of view.

Subject headings: galaxies: clusters: individual (Abell 1795) — galaxies: elliptical and lenticular, cD — galaxies: photometry — galaxies: stellar content

1. INTRODUCTION

The final fate of the cooling gas seen by X-ray telescopes in clusters of galaxies has long been sought, and any system that can provide evidence for star formation arising in a system of cooling gas is of great interest. The cD galaxy in Abell 1795 ($z = 0.0634$) has been an object of much study since it was identified with the radio source 4C 26.42 (Merkelijn 1972) and later found to reside in a cluster cooling flow (McKee et al. 1980). Subsequent optical studies (Sargent 1973; Heckman 1981) found it to possess extended nuclear emission-line gas ($d \sim 20$ kpc, $H_0 = 75$, $q_0 = 0.1$). Spectroscopic studies in both the ultraviolet and optical reveal an unusual blue continuum (Hu 1992; Allen 1995), the structure of which has been recently traced in broadband optical imaging (McNamara & O'Connell 1992). These properties have made it one of the best candidate galaxies for exhibiting star formation arising from a cluster cooling flow, although other mechanisms can be invoked to explain the radio emission and emission-line gas.

Hubble Space Telescope (*HST*) observations, improved CCD sensitivity at blue wavelengths, and the ultraviolet telescopes on board the Space Shuttle during the Astro-2 mission have made this galaxy an object of renewed interest (McNamara & O'Connell 1993; McNamara et al. 1996a; Pinkney et al. 1996). These recent observations have revealed regions with colors bluer than normal [$(U-I) \sim 2.1$; McNamara & O'Connell 1993] for an expected old stellar population, near the galaxy nucleus that may be the sites of recent star formation. These blue regions are confined to the very central ($r \lesssim 20''$) region of the galaxy. The cD appearance at long wavelengths ($\lambda > 7000$ Å), where the light is dominated by the oldest stars, is smooth and does not suggest that a recent globally disturbing event (e.g., a major galaxy interaction) has occurred to trigger a burst of central star formation. Suggested possible triggers for the star formation have included radio jets, collision with a smaller galaxy (McNamara et al. 1996a), and the interaction of the gas cooling out of the X-ray halo with the galaxy interstellar medium (ISM). Each of these interpretations predicts some recent star formation in the galaxy nucleus, but with potentially differing morphologies, resultant population mixes, and emission-line properties.

If the galaxy has undergone recent star formation, then it is natural to turn to the ultraviolet part of the spectrum for observational confirmation. Young stars will most easily be distinguished from the preexisting stellar population by observations shortward of the 4000 Å break. In particular, observations by the Ultraviolet Imaging Telescope (UIT) in its far-UV filter may be used as a valuable diagnostic for stars that are extremely hot ($T_{\mathrm{eff}} \gtrsim 10{,}000$ K). At the distance of the cD ($z = 0.0634$), as few as 1200 O stars would

be detectable with UIT (provided there was no obscuration by dust). At the wavelengths observed by the UIT, all of the underlying old population (primarily G, K, and later type stars) will be invisible, with the important possible exception of extreme horizontal branch (EHB) stars (Ferguson et al. 1991; Dorman, O'Connell, & Rood 1995).

In § 2, we discuss the UIT data and photometry, as well as archival data used in the analyses. We follow in § 3 with a discussion of the implications these new UV data have for star formation properties in Abell 1795.

2. OBSERVATIONAL DATA

In Figure 1 (Plate 6), we present our image obtained with the UIT during the Astro-2 Space Shuttle mission of 1995 March. The UIT took several exposures using a far-UV filter with $\lambda_c = 1520$ Å; $\Delta\lambda = 356$ Å (which we shall hereafter denote by the first two digits of its central wavelength). For this study, we used only the deepest (1310.5 s) exposure. For a complete description of the instrument and preliminary data reduction steps involved, see Stecher et al. (1992). The UIT has a large field of view (40′ diameter), so the entire cluster core was imaged, but little beyond the cD itself was detected. The nominal stellar point-spread function (PSF) for the UIT has an FWHM of $\sim 3''$, but the Abell 1795 images have poorer resolution with FWHM of the stellar PSF of $\sim 6''.8$. Several factors can contribute to decreased resolution, the most common of which is crew motions on board the shuttle during the observation. In § 2.3, we briefly discuss objects other than the cD in the UIT image.

We have also assembled a collection of archival data to complement our UIT observations of this cluster. These additional data, when combined with that from UIT, create a unique, long-wavelength lever arm with which to examine the star formation properties. We extracted two pipeline calibrated image data sets, taken with the F555W (*HST* "V") and F702W filters, from the *HST* archives (u2630401-6). After correcting the image headers for updated WFPC2 astrometry (Hu 1996, private communication), we removed the cosmic rays and applied a charge transfer correction as outlined in Holtzman et al. (1995), and we combined the two longest exposure images (800 s each). Since the portion of the cD galaxy seen by the UIT is the central $\sim 20''$, we used only that portion of the *HST* data (PC chip). No sky subtraction was performed on the *HST* images because the short exposure times (800 s) combined with small pixel size imply that there is little if any contribution to the F555W and F702W signal from a background.

B. McNamara kindly provided us with a copy of his calibrated *U*-band image obtained with the Kitt Peak National Observatory's 2.1 m telescope (McNamara & O'Connell 1992). For comparing the global stellar population with that of the electrons responsible for the radio emission, we acquired a copy of previously published VLA data from J. P. Ge (Ge & Owen 1993).

2.1. *Morphology*

One of the primary goals of the UIT was to investigate the changes in galaxy morphology with wavelength for a variety of galaxy types. As part of this effort, we have constructed a series of figures comparing the UIT image of the cD galaxy with those from other passbands (Figs. 2, 3, and 4 [Pls. 7–9]). These figures show that the UIT image resembles the Hα emission more nearly than the broadband optical emission, and that the UV morphology has no obvious link to the radio morphology. The similarity of the UV and Hα morphologies prompted us to estimate the amount of Lyα contamination in our UIT filter band. To determine the strength of any Lyα emission from the center of the galaxy, we extracted an archival *IUE* spectrum of the cD galaxy (Hu, Cowie, & Wang 1985) and convolved it with the UIT filter response curve. Though the system exhibits moderately strong Lyα emission (see § 2.2), this contributes little to the UIT measured flux. Moreover, Astro-2 Hopkins Ultraviolet Telescope spectra show that those emission lines that are present in the UIT filter are weak and do not contribute substantially to the overall UV flux (Dixon 1996, private communication). Thus, despite the superficial resemblance of the UIT cD image to the Hα morphology, we conclude that the light is from a continuum source and not extended emission-line gas.

Direct comparison of the *HST* optical and UIT UV morphologies is complicated to interpret because of the great difference in resolution. However, the presence of the dust lane dramatically revealed in the *HST* data (Fig. 3) is reflected in the pinching of the UV contours in the UIT image. In general, the UV morphology is much less regular than the *HST* F555W and F702W morphologies. The blue lobes seen by McNamara & O'Connell (1993) may be associated with the north and south peaks of the UV contours separated by $\sim 10''$, but we do not find these regions to be bluer than the galaxy as a whole (in 1520 Å $- V \equiv 15 - V$). The 3.6 cm and 1520 Å morphologies of the cD galaxy are coaligned roughly north-south (Fig. 4). McNamara & O'Connell (1993) found the blue lobes at the ends of the radio emission, leading them to posit that the jets may be inducing star formation via interaction with the galaxy ISM. The UV data suggest very weak concentrations in flux near the outer edges of the radio emission.

To further investigate the morphology of the UV light, we compare its surface brightness profile (Fig. 5) with those at longer wavelengths. We generated surface brightness profiles in the UV, F555W, and F702W bands using the STSDAS ELLIPSE task (Fig. 6), and fitted a function to the profile in McNamara & O'Connell (1993) for the *U* profile. There is no evidence for a point-source component to the UV surface brightness profile. We fitted both elliptical ($r^{1/4}$ law) and disk galaxy (exponential) light profiles to the UIT data, and find that the disk galaxy light profile is a better match. Table 1 gives the results for our model galaxy profile fits. We also performed fits to the F702W profile. The best fit was achieved with a combined point-source, exponential disk, and $r^{1/4}$ law bulge model. However, the disk central surface brightness for this fit is more than 2 mag brighter than the corresponding characteristic bulge surface brightness (I_e), indicating that the central region ($r < 8''$) of the cD has a predominantly disklike light distribution. Thus, both the UV and visual light from the central portion of the galaxy are better characterized by exponential light distributions than by elliptical galaxy light distributions, but with the UV light being more extended ($r \sim 20''$). Interestingly, Hu et al. (1985) found spectroscopic evidence for emission-line gas rotation in the central part of the cD, while Anton (1993) found no evidence for a rotating disk; however, neither measurements were sensitive to the small spatial scales accessible to *HST*, nor to the young stellar population easily isolated by the UIT.

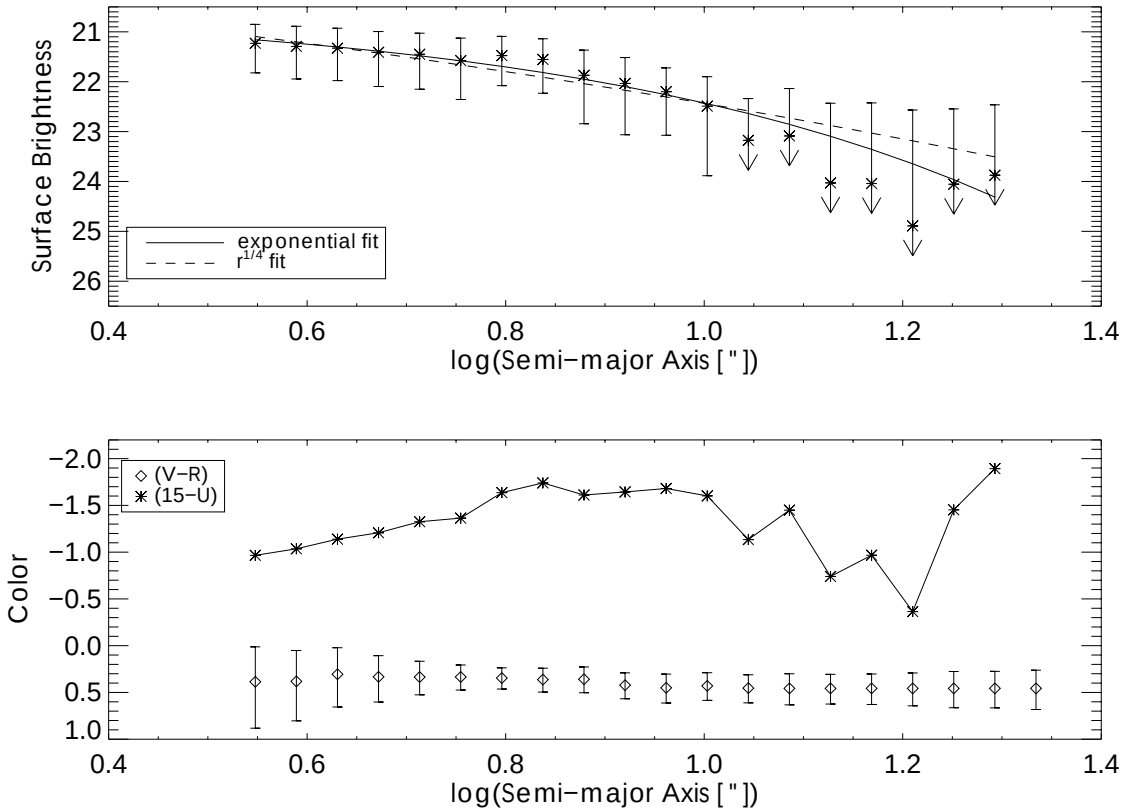

FIG. 5.—*Top*: Surface brightness profile (magnitudes arcsec^{-2}) in the 1520 Å band, along with best-fitting disk and elliptical galaxy models. *Bottom*: Color profiles for the galaxy over the region defined by the surface brightness profile.

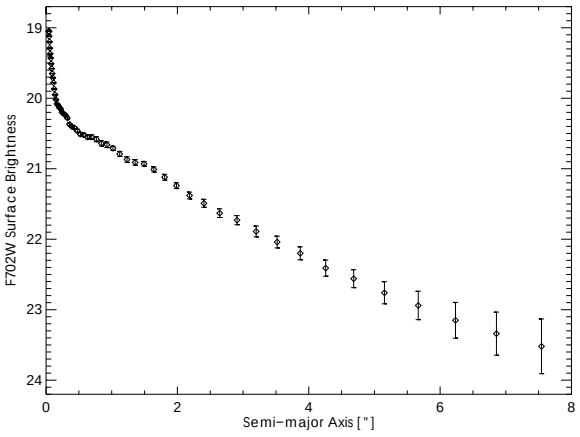

FIG. 6.—Surface brightness profile (magnitudes arcsec^{-2}) for the *HST* F702W image of the central part of Abell 1795.

The $V-R$ color index does not vary significantly over the central portion of the cD. However, the $(15-V)$ index changes with the central part being slightly redder than the outer parts. This is most likely a result of the presence of the dust so easily visible in the *HST* image. O'Connell et al. (1992) found that several ellipticals observed with UIT generally become bluer with decreasing radius, but none of those galaxies were know to possess significant amounts of centrally concentrated dust.

2.2. *cD Galaxy Photometry*

We performed our photometry using software specifically tailored to UIT data, but modeled on the DAOPHOT aperture photometry routine. Curve-of-growth analysis shows that the cD galaxy light (centered at $\alpha = 13^h48^m52^s.42$, $\delta = +26°35'34''.7$) is contained within a circle of radius $\sim 25''$. The aperture magnitude and corresponding

TABLE 1

SURFACE BRIGHTNESS PROFILE MODELS

Model	Scale Length[a]	χ^2
UV: Disk	4.5 ± 0.3	5.4
UV: $r^{1/4}$-law	41.1 ± 16.6	183
R: Disk[b]	3.7 ± 0.04	4.9
R: $r^{1/4}$ law[b]	142 ± 32	42.7
R: (composite) Disk + $r^{1/4}$ law + point source	...	0.54
R (composite) Disk component	2.2 ± 0.3	...
R (composite)$r^{1/4}$-law component	0.3 ± 0.1	...

[a] Scale length is in units of arcseconds.

[b] Fits performed over $0''.3 < r < 8''$ region of profile to exclude the central peak in the *HST* profile.

flux for the galaxy are $m_{15} = 15.54 \pm 0.09$ (2.21×10^{-15} ergs s^{-1} cm^{-2} Å^{-1}). Henceforth, all photometric comparisons will be confined to this region or specific apertures within this radius. Using archival *IUE* spectra, we are able to estimate the contribution to the UIT flux arising from the Lyα emission in the galaxy (see also Hu 1992). We have corrected the UIT magnitudes by $\Delta m_{15} = 0.08$ to account for this emission-line contribution, yielding $m(\text{continuum})_{15} \equiv m_{c,15} = 15.62 \pm 0.09$. There was no detectable UV flux associated with the blue filamentary region described by McNamara & O'Connell (1993). To check for the presence of the blue lobes, we placed small ($5'' \times 5''$) apertures on the locations of lobes (from McNamara & O'Connell 1993, see their Fig. 6) and on the galaxy center. We find no significant difference between the colors in these various regions. However, the low spatial resolution of the UIT image and typical uncertainty in its photometry ($\sim$0.1 mag), folded in with stochastic variations of the spatial distribution of O stars, imply that detecting color difference with these images would be difficult.

We photometered the *HST* and *U*-band data within the same region, and the resulting magnitudes and colors are listed in Table 2. Steps outlined in Holtzman et al. (1995) were taken to calibrate the *HST* photometry. For both the *U* and *HST* images, we digitally removed a small elliptical galaxy at $r \sim 9''.5$, replacing the pixels with those from a region at the same radius but 180° different in position angle. The *HST* magnitudes were corrected for emission-line contributions using the data from Anton (1993). These corrections were small, with $\Delta V = 0.02$ and $\Delta R = 0.06$, respectively. The only emission line in the *U*-band filter is the line [O II] λ3727, for which we correct by $\Delta U = 0.04$. The optical magnitudes have been *K*-corrected using the models from Coleman, Wu, & Weedman (1980). We estimated the *K*-correction for the 1520 Å ($K_{15} = 0.26$) by convolving a numerically redshifted O star spectrum with the UIT filter response and comparing this with its $z = 0$ counterpart. No corrections for Galactic extinction have been applied because $E_{B-V} \lesssim 0.01$.

We also photometered a polygonal region ($\sim 8'' \times 4''$) centered on the dust lane and visible within the *HST* image to compare the colors inside and outside this region. The change in color compared with an identical region centered on the optical nucleus is $\Delta(15 - V) = 0.8$.

2.3. *Other Objects*

There are 10 previously cataloged objects, excluding the cD galaxy, visible in the UIT image. Five of these are cataloged only in the *HST* Guide Star Catalog (GSC), while the other five are SAO 82997 [$m_{15} = 14.00 \pm 0.07$, $(15 - V) = 4.89$, F8V], SAO 83004 [$m_{15} = 14.30 \pm 0.10$, $(15 - V) = 4.97$, F0V], Abell cluster galaxies 40 and 151 (Huchra et al. 1990), and 1345.6 + 2639 [$m_{15} = 15.85 \pm 0.10$, $(15 - V) = 0.15$; a Seyfert galaxy]. The two stars and the Seyfert galaxy are all point sources. There is no previously published photometry for the two cluster galaxies, but we have estimated their colors based on their digitized Palomar Sky Survey (DPOSS) images. We find the following: Abell 40 [$m_{15} = 16.4 \pm 0.2$, $(15 - V) = 3.0$] and Abell 151 [$m_{15} = 16.6 \pm 0.2$, $(15 - V) = 2.3$]. These magnitudes have not been corrected for *K*-dimming or for extinction (Galactic or intrinsic). Both objects are quite blue for normal cluster galaxies and may be experiencing some star formation. Assuming their UV light is the result of young stars, we estimate that Abell 40 and Abell 151 contain $\sim$8500 O stars. This would imply star formation rates of approximately 1 $M_\odot$ yr^{-1}. We note, however, that their $(15 - V)$ colors are similar to those seen in galaxies with "UV upturns" arising from hot EHB stars in the old population (Dorman et al. 1995). Therefore, without other evidence for recent star formation (Hα emission, for example) we cannot distinguish between young stars and EHB stars as the primary cause for blue colors.

In addition to these sources, there are four uncataloged sources (all are 5 σ detections) with mean magnitude $\langle m_{15} \rangle = 16.7$. Comparison of their positions with the DPOSS suggests that all of these are stars or groups of stars too faint in the visible to be included in the *HST* GSC. Comparison with deep optical images has proved to be fruitful in identifying faint UIT sources (O'Neil et al. 1996) that are easily overlooked on the POSS. We expect the same may be true for this image, since there are several faint (2–3 σ) sources without optical counterparts in the DPOSS.

TABLE 2

PHOTOMETRIC PROPERTIES

Parameter	Value
$m_{c,15}$	15.36 ± 0.07
$15 - U$	−0.18
$15 - V$	0.53
$V - R$	0.61

NOTES.—All properties measured within $r = 12''$ aperture. Values include *K*-corrections (see § 2.2).

3. DISCUSSION AND SUMMARY

To estimate the star formation history or current star formation rate using the UV measurements from UIT, we must first determine the nature of the UV light. If the light arises primarily from emission-line gas, then it will tell us little about massive star formation. Early *IUE* spectroscopy by Nørgaard-Nielsen, Jørgensen, & Hansen (1984) suggested that the UV light was the result of high-temperature gas, but later, *IUE* observations measured a continuum (Hu 1992; Crawford & Fabian 1993). Moreover, recent optical spectroscopy has found strong evidence of a hot continuum (Allen 1995) at optical wavelengths. Spectroscopy at all wavelengths reveals line ratios from the emission-line gas that are inconsistent with ionization via a nuclear, nonthermal power-law source. The LINER-like spectrum of Abell 1795 is better fitted by shock models (van Breugel, Heckman, & Miley 1984; Hu 1992; Anton 1993) or photoionization by a hot population (Allen 1995). Thus, it seems likely that the bulk of the UV emission in the UIT bandpass comes from a continuum of hot stars that may, in turn, be responsible for ionizing some of the emission-line gas.

3.1. *Star Formation*

Since at least some portion of the observed Hα and Lyα flux arises from gas photoionized by a UV continuum, there must be a significant population of young hot stars, implying either a recent episode of star formation ($t \sim 3$ Myr) or continuous star formation. The UIT magnitude listed in Table 2 implies a luminosity at 1500 Å, $L_{1500} = 1.9 \times 10^{42}$ ergs s^{-1}. We can estimate the number of O5 stars required to produce the measured UIT flux and then compare that

with the expected star formation rate needed to fuel the Hα emission. Using Kurucz model atmospheres (Kurucz 1993), assuming an effective temperature and luminosity of 38,000 K, $\log (L_{\rm bol}/L_{\odot}) = 5.7$ for a mid-O star, and cosmology with $H_0 = 75$, $q_0 = 0.1$, we require 1.8×10^4 stars to match the UIT, K-corrected flux. This represents the *minimum* number of ionizing stars because no extinction correction has been applied and mid-O stars produce more ionizing flux than early B stars. Without ultraviolet spectroscopic information, we cannot restrict further the relative contributions of various stellar types with temperatures greater than 15,000 K to the UIT flux. Adopting the extinction ($E_{B-V} = 0.14$) from Hu (1992), and assuming a Galactic extinction law (Savage & Mathis 1979) and foreground screen dust model, causes the estimated number of O stars to rise to 5.3×10^4. Recent optical spectroscopy by Allen (1995) predicts 2.4×10^4 O stars (adjusting to our cosmology) using similar extinction, suggesting that the screen model may be a reasonable approximation for the dust extinction in the galaxy center. The implied star formation rate (SFR) is in the range 8–23 $M_{\odot}$ yr^{-1}, depending on the IMF model, with the lower bounds corresponding to a Kennicutt (1983) IMF and the upper bound corresponding to a Miller & Scalo (1979) IMF. Since some of the Hα emission comes from shocked gas, an SFR that is derived assuming that all of the emission comes from photoionized gas is an upper limit. Therefore, it is likely that the actual SFR is closer to the lower limit in the case of Abell 1795. This SFR is consistent with the predicted star formation rates one calculates from the Hα luminosity (5 $M_{\odot}$ yr^{-1}; van Breugel et al. 1984; Kennicutt 1983). These star formation rates are substantially lower than those estimated from recent X-ray analyses ($\sim$300 $M_{\odot}$ yr^{-1}; Edge, Stewart, & Fabian 1992; Fabian 1994).

To further test the various scenarios for possible star formation histories, we use models based on the following: (1) a single, instantaneous burst of star formation; (2) a single, exponentially decaying burst of star formation; (3) continuous, constant star formation; and (4) a single, instantaneous old burst with smaller, younger bursts superimposed. The first three models are described in more detail in Cornett et al. (1994). The fourth model is simply a scaled superposition of the models in item (1). We have plotted color-color diagrams using the four colors, $(15 - V)$, $(15 - U)$, $(U - V)$, and $(V - R)$, for each set of the above models to compare with the global colors of the cD galaxy (Fig. 7). The colors have been corrected for K-dimming but not extinction. Extinction vectors based on various models for the distribution of the dust are added to the plot. Several models for the star formation history can be ruled out. Models with exponentially decaying star formation, as well as those in which the central population was created in a single burst of age greater than about a few hundred million years, have broadband colors too red to match the cD. Models with some levels of continuous star formation and/or those with recent bursts, however, can reproduce the colors. The most plausible burst model is one in which an old galaxy ($z_{\rm form} = 5$) experiences a Salpeter IMF burst of

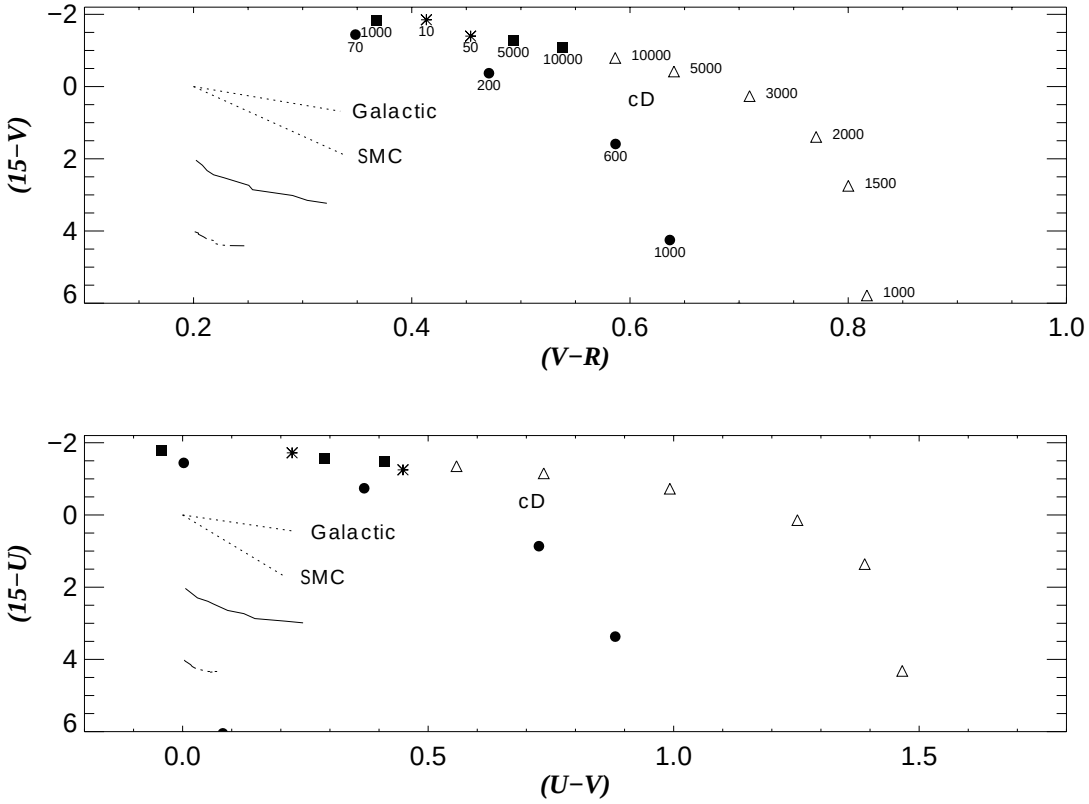

FIG. 7.—Color-color diagrams showing the location of the cD along with several models of star formation histories. Symbols have the following meaning: (*filled circles*) Single generation, instantaneous bursts of star formation with the age of the burst (in Myr) under the symbol; (*open triangles*) single generation, exponentially decaying star formation with the decay time (Myr) next to the symbol; (*open squares*) constant, continuous star formation, beginning at the time listed under the symbol; (*stars*) single, 4 Myr old burst added to an old population (see § 3.1); and ("cD") Abell 1795 measured colors. Tracks indicating the effects of extinction are superimposed (see § 3.2). The errors in the cD colors are smaller that the letters used to label the point itself.

age 4 Myr and total mass 25% of the old population, within the photometered aperture. We estimated the mass interior to $r = \sim 25''$ by comparing the fraction of light within this radius for an $r^{1/4}$ law galaxy with its total, and we assumed a constant M/L ratio of 20. Since this likely underestimates the central M/L ratio, the mass required of our burst to match the cD colors is an upper limit. The most plausible continuous, constant star formation model that matched the far–UV-visible colors is one in which the galaxy has been forming stars at a rate ~ 5–$10\, M_{\odot}\ \mathrm{yr}^{-1}$ over the past 5 Gyr.

3.2. *Dust Extinction*

The dust lane visible in Figure 3 complicates the interpretation of broadband observations, particularly those involving ultraviolet light. By comparing the measured *IUE* Lyα flux to Hα flux, and assuming suitable values for the intrinsic line flux ratio, Hu (1992) estimated the intrinsic $E_{B-V} = 0.14$ but with a wide possible range ($0.2 < E_{B-V} < 0.22$). Recent optical spectroscopy by Allen (1995) suggests $E_{B-V} = 0.22$. The straight line vectors in Figure 7 show the effects of dust assuming both the Galactic Savage & Mathis (1979) ($A_{1520} = 8.32 E_{B-V}$) and SMC extinction laws. The curved lines (for a dusty galaxy, similar to a spiral and an elliptical galaxy model) are the extinction curves based on the dust/stellar distribution models of Witt, Thronson, & Capuano (1992). Their models of mixed dust, gas, and stars generally produce smaller extinction in the UV than simple foreground screen models. The location of the galaxy in the color-color diagrams is consistent with systems having continuous star formation over the last 5–10 Gyr when combined with the $E_{B-V} = 0.14$, Galactic-law screen or dusty galaxy extinction models, or with a system characterized by an old population with a 2–5 Myr burst and the same extinction laws. Extinction laws with $E_{B-V} = 0.22$ combined with measured cD colors generally produce values too blue to be consistent with any of our galaxy models.

3.3. *Conclusions*

Our analyses reveal several things. The light at 1520 Å is best characterized by an exponential or disklike light profile with a scale length of 4 kpc. Similarly, the F702W light is best matched by a predominantly disklike profile, but with scale length of 2 kpc. The UV-optical colors match those of models with continuous star formation for $t \sim 5$–10 Gyr or those of an old galaxy with a massive, young ($t \sim 4$ Myr) burst. Both of these properties are consistent with the UV light coming from an accreted population formed in a cluster cooling flow or from an episode of star formation induced by an interaction with a much smaller galaxy. The cooling flow scenario has the following points as supporting evidence: (1) line ratios indicative of shock heated gas, and (2) the inner surface brightness profile does not show significant disturbances in the UV or optical bands. However, detailed image analyses of deep *U*-imaging by McNamara et al. (1996b) appears to have revealed possible debris associated with an interaction of the cD with two small galaxies. These features are too faint to have been detected with the UIT. High-resolution images in the UV would help constrain further the nature of the UV bright population.

We wish to thank Brian McNamara for providing us with a *U*-band image of Abell 1795. E. P. S. also thanks Jason Pinkney for helpful comments about photometry of *HST* images. This research has made use of the NASA/IPAC Extragalactic Database (NED), which is operated by the Jet Propulsion Laboratory, California Institute of Technology, under contract with the National Aeronautics and Space Administration.

REFERENCES

Allen, S. W. 1995, MNRAS, 276, 947
Anton, K. 1993, A&A, 270, 60
Coleman, Wu, C. C., & Weedman, D. 1980, ApJ, 43 393
Cornett, R. H., et al. 1994, ApJ, 426, 553
Crawford, C. S., & Fabian, A. C. 1993, MNRAS, 265, 431
Dorman, B., O'Connell, R. W., & Rood, R. T. 1995, ApJ, 442, 105
Edge, A. C., Stewart, G. C., & Fabian, A. C. 1992, MNRAS, 258, 177
Fabian, A. C. 1994, AR&A, 32, 277
Ferguson, H. C., et al. 1991, ApJ, 381, L69
Ge, J. P., & Owen, F. N. 1993, AJ, 105, 778
Heckman, T. M. 1981, ApJ, 250, L59
Holtzman, J., et al. 1995, PASP, 107, 1065
Hu, E. M. 1992, ApJ, 391, 608
Hu, E. M., Cowie, L. L., & Wang, Z. 1985, ApJS, 47, 447
Huchra, J., et al. 1990, ApJS, 52, 89
Kennicutt, R. C. 1983, ApJ, 272, 54
Kurucz, R. 1993, CD-ROM, No. 13
McKee, J. D., Mushotzky, R. F., Boldt, E. A., Holt, S. S., Marshall, F. E., Pravdo, S. H., & Serlemitsos, P. J. 1980, ApJ, 242, 843
McNamara, B. R., Jannuzi, B. T., Elston, R., Sarazin, C. L., & Wise, M. 1996a, ApJ, 469, 66
McNamara, B. R., & O'Connell, R. W. 1992, ApJ, 393, 579
———. 1993, AJ, 105, 417
McNamara, B. R., Wise, M., Sarazin, C. L., Jannuzi, B.T., & Elston, R. 1996b, ApJ, 466, L9
Merkelijn, J. K. 1972, Australian J. Phys., 25, 451
Miller, G. E., & Scalo, J. M. 1979, ApJS, 41, 513
Nørgaard-Nielsen, H. E., Jørgensen, H. E., & Hansen, L. 1984, A&A, 135, L3
O'Connell, R. W., et al. 1992, ApJ, 395, L45
O'Neil, K., Bothun, G. D., Smith, E. P., & Stecher, T. P. 1996, AJ, 112, 431
Pinkney, J., et al. 1996, BAAS, 27, 1443
Sargent, W. L. W. 1973, ApJ, 182, L13
Savage, B. D., & Mathis, J. S. 1979, ARA&A, 17, 73
Stecher, T. P., et al. 1992, ApJ, 395, L1
van Breugel, W., Heckman, T., & Miley, G. 1984, ApJ, 276, 79
Witt, A., Thronson, H. A., Jr., & Capuano, J. 1992, ApJ, 393, 611